

Bandgap Engineering in High-Efficiency Multijunction Concentrator Cells

R. R. King, R. A. Sherif, G. S. Kinsey, S. Kurtz¹, C. M. Fetzer, K. M. Edmondson,
D. C. Law, H. L. Cotal, D. D. Krut, J. H. Ermer, and N. H. Karam
Spectrolab, Inc., Sylmar, CA

¹National Renewable Energy Laboratory, Golden, CO

ABSTRACT

This paper discusses semiconductor device research paths under investigation with the aim of reaching the milestone efficiency of 40%. A cost analysis shows that achieving very high cell efficiencies is crucial for the realization of cost-effective photovoltaics, because of the strongly leveraging effect of efficiency on module packaging and balance-of systems costs. Lattice-matched (LM) GaInP/ GaInAs/ Ge 3-junction cells have achieved the highest independently confirmed efficiency at 175 suns, 25°C, of 37.3% under the standard AM1.5D, low-AOD terrestrial spectrum. Lattice-mismatched, or metamorphic (MM), materials offer still higher potential efficiencies, if the crystal quality can be maintained. Theoretical efficiencies well over 50% are possible for a MM GaInP/ 1.17-eV GaInAs/ Ge 3-junction cell limited by radiative recombination at 500 suns. The bandgap – open circuit voltage offset, $(E_g/q) - V_{oc}$, is used as a valuable theoretical and experimental tool to characterize multijunction cells with subcell bandgaps ranging from 0.7 to 2.1 eV. Experimental results are presented for prototype 6-junction cells employing an active ~1.1-eV dilute nitride GaInNAs subcell, with active-area efficiency greater than 23% and over 5.3 V open-circuit voltage under the 1-sun AM0 space spectrum. Such cell designs have theoretical efficiencies under the terrestrial spectrum at 500 suns concentration exceeding 55% efficiency, even for lattice-matched designs.

1. Introduction

Multijunction concentrator solar cells[1-3] for terrestrial applications have reached the point at which the next set of technology improvements are likely to push efficiencies over 40%. Very high solar cell efficiencies are crucial to the cost-effective commercialization of concentrator and flat-plate photovoltaic systems alike[4-8], because of the highly leveraging effect that efficiency has on module packaging and balance-of-system costs. This paper discusses the semiconductor device research paths being investigated with the aim of reaching the 40% efficiency milestone and higher.

A central theme for many of these research thrusts is to change the partition of the solar spectrum afforded by the subcell bandgaps in multijunction cells, to one more advantageous for efficient energy conversion. To this end, lattice-mismatched, or metamorphic, subcell materials, unconventional alloys such as GaInNAs, and cell structures with more than 3 junctions are being investigated with the goal of exceeding 40% solar cell efficiencies.

2. Motivation – PV Concentrator Economics

An important question that motivates much of the strategy in photovoltaic research is "Why hasn't photovoltaic electricity generation become widespread to date?" A widely-referenced and very useful cost study by Swanson that helps to answer this question can be found in [8]. In that paper, a wide variety of flat-plate and concentrator PV technologies are evaluated for their economic effectiveness.

We adapted the methodology in [8] for a slightly different purpose, to find the dependence of the cost effectiveness of a photovoltaic system on the cell cost per unit area, in order to determine the suitable range of cell cost. Using a simple expression given in Fig. 1, the PV system cost per kWh over a 5 year payback period was calculated as a function of cell cost per unit area, taking into account: typical module packaging, tracking, balance-of-system (BOS), and similar costs documented in [8]; module optical efficiency and cost differences for flat-plate and concentrator systems; the ability to use the global and direct solar resource for flat-plate and concentrator systems; in addition to the variable cell cost. The resulting curves of the average cost of electricity in \$/kWh generated by the system in 5 years, plotted in Fig. 1, show that both flat-plate and concentrator systems can reach electricity costs below a near-term target value of 0.15 \$/kWh for at least some combinations of high efficiency and low cell cost.

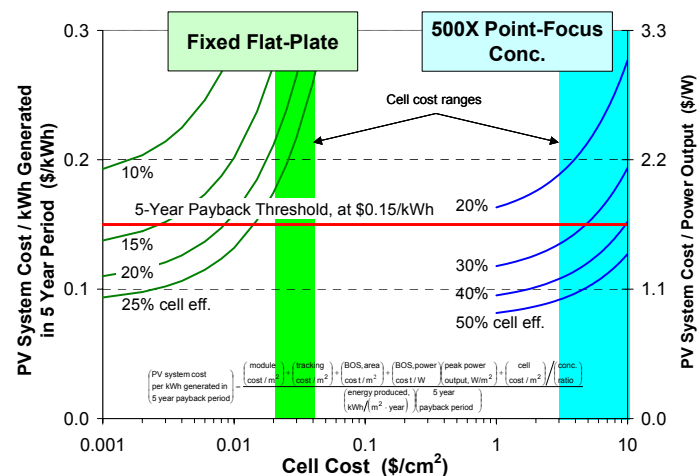


Figure 1. Average cost of electricity produced over a 5 year payback period, in \$/kWh, as a function of cell cost per unit area. Two distinct domains can be seen: flat-plate systems which require very low cell cost to be cost effective, and concentrator systems which can tolerate high cell cost.

Two families of curves are evident in Fig. 1: those for flat-plate systems for which very low cell costs are required, and those for concentrators for which relatively high cell costs can be tolerated. Note that below about 12% efficiency for flat-plate, and about 20% efficiency for concentrator systems, a PV system cannot become cost effective in 5 years even for zero cell cost, due to the cost of module packaging, BOS, and similar costs. Cost effective flat-plate systems need to be in the range of 0.1-1.0 cents per cm^2 cell cost for 20%-efficient cells, while for concentrator systems with 30%-efficient cells, a cell cost of 1-5 dollars per cm^2 , or 500-1000 \times greater, is suitable for cost effectiveness. Both efficiency values are reasonable for the two technologies, but using the typical cell cost ranges cited in [8], indicated in Fig. 1, it can be seen that the challenge for flat-plate technologies is to reduce present typical cell costs of 0.02-0.04 $\text{\$/cm}^2$ by an order of magnitude, maintaining cell efficiencies of 20%, while for concentrator systems 30% cells are cost effective now, and the challenge is to reach higher efficiencies in the 40-50% range for greater cost effectiveness.

A large part of the answer to the question posed at the beginning of the section is that solar energy is a dilute resource, and low-efficiency systems require very large areas of glass, metal, and plastic needed for module packaging, support structures, wiring, etc. Even without considering the cost of semiconductor materials, the costs of those relatively mundane materials over large areas can preclude cost effectiveness. Fortunately, high-efficiency solar cells strongly reduce the module area needed for a given electric power output, and strongly leverage module and BOS costs, and with the use of $\sim 500\times$ concentration, relatively high cell costs per area can be tolerated. Taking cell efficiencies into the 40-50% range may well be the clearest path to photovoltaic cost effectiveness.

3. Cell Designs and Theoretical Efficiency

Multijunction Cell Architectures

The division of the solar spectrum by the 1.8 eV/ 1.4 eV/ 0.67 eV combination of bandgaps in a lattice-matched (LM) GaInP/ GaInAs/ Ge 3-junction cell leads to excess photogenerated current density in the Ge subcell. Part of this wasted current can be used effectively in the middle cell if its bandgap is lowered, as in lattice-mismatched, or metamorphic (MM) GaInP/ GaInAs/ Ge 3-junction cells with a 1.2-1.3 eV GaInAs middle cell [1, 9-15]. The challenge then becomes to maintain low Shockley-Read-Hall (SRH) recombination due to defects in these mismatched materials.

Higher lattice mismatches give still greater advantages if the crystal quality can be maintained. Studies of highly-lattice-mismatched single-junction GaInAs cells were conducted with indium compositions ranging from 0% to 35% indium content in 0.95-eV $\text{Ga}_{0.65}\text{In}_{0.35}\text{As}$ cells with 2.4% lattice mismatch to the Ge substrate[1].

Minority-carrier properties of these mismatched GaInAs materials and GaInP at the same lattice constant were explored. At a bandgap of 1.1 eV, GaInAs cells with 1.6% lattice mismatch have nearly the same open-circuit voltage as record efficiency silicon solar cells at the same bandgap, indicating the degree to which defects have been suppressed by optimization of the step-graded buffers in these metamorphic devices. The dislocation density in these $\text{Ga}_{0.77}\text{In}_{0.23}\text{As}$ materials is $3\text{-}4 \times 10^6 \text{ cm}^{-2}$, as measured by plan-view TEM and cathodoluminescence[1]. TEM imaging over a large sample area indicates a dislocation density of only $2 \times 10^6 \text{ cm}^{-2}$ for $\text{Ga}_{0.65}\text{In}_{0.35}\text{As}$ with $\sim 0.95\text{-eV}$ bandgap, consistent with the observation that the minority-carrier lifetime measured by time-resolved photoluminescence (TRPL) is about 10 ns for both the 1.1- and 0.95-eV materials[1]. These metamorphic materials enable advanced multijunction cell designs incorporating a 0.9-1.1 eV subcell.

Work in this area has yielded cell results on metamorphic $\text{Ga}_{0.44}\text{In}_{0.56}\text{P}/ \text{Ga}_{0.92}\text{In}_{0.08}\text{As}/ \text{Ge}$ 3-junction cells, with the upper two cells having a lattice constant 0.5% larger than the Ge substrate [1,9]; $\text{Ga}_{0.35}\text{In}_{0.65}\text{P}/ \text{Ga}_{0.83}\text{In}_{0.17}\text{As}$ cells [7]; 2- and 3-junction $\text{Ga}_{0.29}\text{In}_{0.71}\text{P}/ \text{Ga}_{0.77}\text{In}_{0.23}\text{As}/ \text{Ge}$ cells [14,15]; and on GaInP/ GaAs/ 1-eV GaInAs 3-junction cells with the upper two subcells lattice matched to a GaAs substrate [16,17]. Schematics of this latter cell design are shown in Fig. 2.

Another way to utilize the excess photogenerated current in the Ge subcell in 3-junction cells is to insert a $\sim 1\text{-eV}$ semiconductor, such as GaInNAs lattice-matched to Ge, above the Ge subcell. 5- and 6-junction cell designs partition the solar spectrum into narrower wavelength ranges than 3-junction cells, allowing all the subcells to be current matched to the low-current-producing GaInNAs subcell. Additionally, the finer division of the incident spectrum reduces thermalization losses from electron-hole pairs photogenerated by photons with energy far above the bandgap energy, and the smaller current density in 5- and 6-junction cells lowers resistive I^2R losses. Cross-sectional diagrams of 5- and 6-junction cells are drawn in Fig. 3.

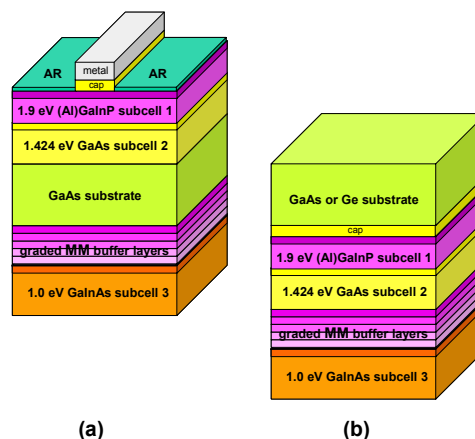


Figure 2. Two configurations of 3-junction solar cells with a highly-lattice-mismatched, inverted 1-eV GaInAs bottom subcell: (a) growth on two sides of a transparent GaAs substrate; (b) growth on the back of a GaAs or Ge substrate that is removed during cell fabrication.

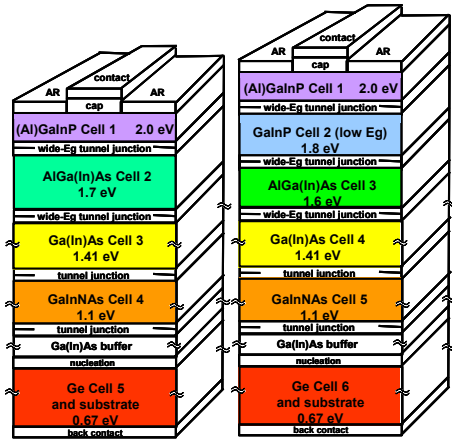


Figure 3. Cross-sections of 5- and 6-junction cells.

At a given lattice mismatch, higher efficiencies can be reached in many multijunction cell designs if the GaInP top cell bandgap is increased, since less light then needs to be leaked through the GaInP to the GaInAs cell beneath, and more can be converted at the higher voltage of the GaInP top cell. The effect of disordering Ga and In atoms on the group-III sublattice, is known to increase the bandgap by ~ 100 meV for the LM case. This effect has been confirmed to persist in lattice-mismatched, In-rich compositions of GaInP as well[11,14]. Use of AlGaInP to raise the top cell bandgap can also increase the multijunction cell efficiency[2,11].

Theoretical efficiency

The theoretical efficiency of multijunction solar cells limited by the fundamental mechanism of radiative recombination was calculated as a function of subcell bandgap in 3- and 6-junction cells, at 25°C. The current density in each subcell was found from the photon flux in each photon energy range of the standard terrestrial AM1.5D, low-AOD spectrum[18], the open-circuit voltage from the carrier concentration at which radiative recombination is in steady state with this photogenerated current density, and the cell efficiency was found by combining the current-voltage characteristics of the subcells in the multijunction stack.

The calculated efficiencies for 3-junction cells are plotted in Fig. 4. The familiar case of a GaInP/ GaInAs/ Ge 3-junction solar cell can be found in the right-hand set of curves. For the lattice-matched case with a 1.41-eV GaInAs subcell 2, the optimum top cell bandgap is about 1.9 eV. As one goes to lower bandgaps for subcell 2, as for MM GaInAs, the optimum top subcell E_g shifts down as well, reaching ~ 1.74 eV at the optimum subcell 2 bandgap of 1.17 eV, for a calculated efficiency over 55%.

For a 1.4-eV subcell 2, a higher efficiency can be achieved with a 1.0-eV bottom subcell than for a Ge subcell, as can be seen in the left-hand set of curves in Fig. 4. The theoretical efficiency for this case with a 1.0-eV subcell 3, corresponding to the cell configurations sketched in Fig. 2, is $\sim 53\%$. Interestingly, as the middle subcell 2 bandgap drops to

1.17 eV, the optimum subcell 3 becomes 0.69 eV, coinciding very closely with the bandgap of Ge, with a calculated efficiency of over 55%.

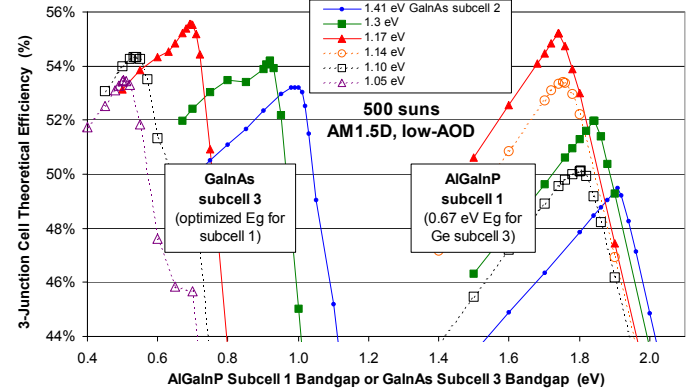


Figure 4. Theoretical efficiency of 3-junction solar cells limited only by radiative recombination, as a function of the bandgap of the (top) subcell 1 material such as AlGaInP, and the (bottom) subcell 3 material, such as Ge, GaInAs, or lattice-mismatched GaInAs.

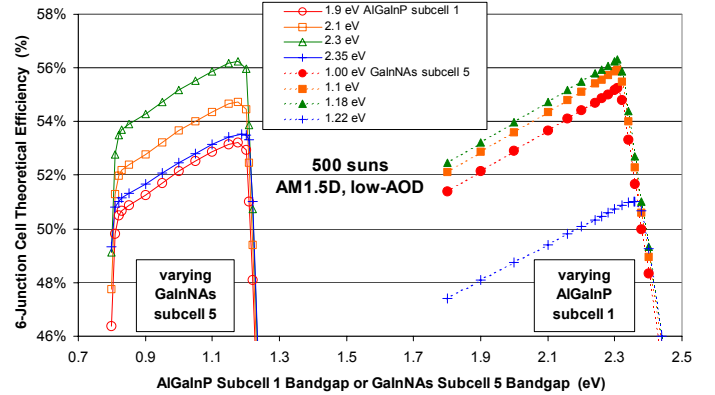


Figure 5: Theoretical efficiency of 6-junction solar cells limited only by radiative recombination, as a function of the bandgap of the (top) subcell 1 material such as AlGaInP, and the subcell 5 material on top of the Ge subcell 6, such as GaInAs, or lattice-mismatched GaInAs.

Figure 5 plots the theoretical efficiency of 6-junction cells under the concentrated terrestrial spectrum, again at 25°C. The bandgaps of subcells 2, 4, and 6 were assumed to be 1.8 eV corresponding to ordered GaInP, 1.41 eV for LM 1%-In GaInAs, and 0.67 for the Ge substrate, respectively. Higher efficiencies are possible for full flexibility in bandgap. For optimum top subcell E_g of 2.3 eV and subcell 5 E_g of 1.18 eV, efficiencies over 56% are possible for a lattice-matched configuration using GaInNAs for subcell 5, or for metamorphic configurations using MM 1.18-eV GaInAs in subcell 5. Subcell 1 bandgaps of 1.9 or 2.1 eV, which are easier to achieve, still yield theoretical efficiencies of 53.2% and 54.7%, respectively.

4. Results and Discussion

Metamorphic semiconductor materials

Internal quantum efficiency (QE) data of metamorphic GaInAs solar cells grown on Ge substrates, with bandgaps ranging from 1.4 to 0.96 eV, are plotted in Fig. 6, showing the progression of the absorption edge with increasing lattice mismatch. Note that the near-bandedge QE remains very high out to 1.08-eV GaInAs, falling only moderately at 0.96 eV, indicating long minority-carrier diffusion lengths given the large lattice-mismatches of 1.6% for 1.08-eV and 2.4% for 0.96-eV GaInAs. These long diffusion lengths result from the long minority-carrier lifetimes measured in these materials[1], and translate into the high open-circuit voltages discussed above.

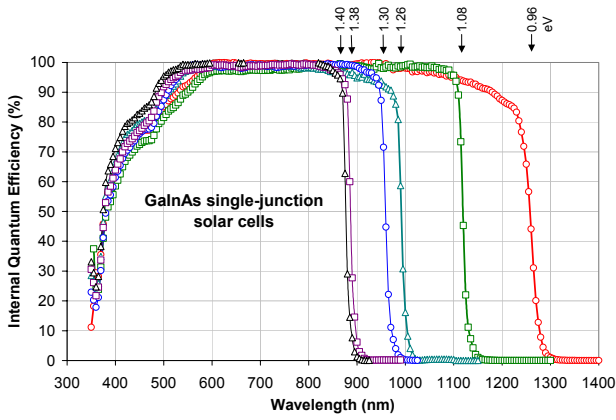


Figure 6. Measured internal QE curves for single-junction GaInAs cells, showing the shift in wavelength corresponding to the bandgap, and strong response near the bandgap wavelength indicating long diffusion lengths in these metamorphic materials.

Bandgap-voltage offset

When investigating semiconductors with a wide range of bandgaps for use in solar cells, a method to gauge the material quality is needed, that can compare non-ideal recombination properties in one material to those in another. The difference between the bandgap voltage $V_g = E_g/q$ and open-circuit voltage V_{oc} , is a useful quick gauge of semiconductor quality for many different materials systems[11]. The smaller this offset voltage $(E_g/q) - V_{oc}$, the closer the electron and hole quasi-Fermi levels are to the conduction and valence band edges, respectively, and the more closely the voltage approaches the fundamental limit set by radiative recombination. This observation is based on the dependence of open-circuit voltage on bandgap in a solar cell in which the only recombination mechanism is radiative:

$$V_{oc} = \frac{kT}{q} \ln \left(\frac{J_{ph}}{qwBn_i^2} \right) \quad (1)$$

$$n_i^2 = N_C N_V e^{-E_g/kT} \quad (2)$$

$$V_{oc} = \frac{E_g}{q} - \frac{kT}{q} \ln \left(\frac{qwB N_C N_V}{J_{ph}} \right) \quad (3)$$

where J_{ph} is the photogenerated current density, w is the thickness of the solar cell base, n_i is the intrinsic carrier concentration, B is the radiative recombination coefficient, and the other symbols have their usual meaning. Note that the logarithmic second term in Eqn. 3 depends only weakly on E_g , resulting in a nearly constant offset voltage $(E_g/q) - V_{oc}$ between the bandgap and the calculated V_{oc} for solar cells limited by radiative recombination, across a wide range of bandgaps. Thus the difference between the measured open-circuit voltage and the V_{oc} predicted in the radiative limit can be used to determine the non-radiative recombination components, primarily Shockley-Read-Hall (SRH) recombination. When typical values for N_C , N_V , B , w , J_{ph} , and their dependences on bandgap are plugged into Eqn. 1, the difference $(E_g/q) - V_{oc}$ varies only from ~0.31 V to 0.39 V in the radiative limit, for bandgaps ranging from 0.95 to 2.0 eV.

One way to visualize the approximate constancy of $(E_g/q) - V_{oc}$ for different semiconductors is that B varies only slowly with E_g , and therefore the pn product in steady state, in which the photogenerated current per unit volume J_{ph}/qw equals the radiative recombination rate Bnp , is roughly similar for a given incident photon flux. Because the density of states in the conduction band is similar for many semiconductors, and the same is true for the valence band, similar p and n among different semiconductors in steady state translates to roughly the same energy difference between the conduction band edge and the electron quasi-Fermi level, and the same is true between the valence band edge and the hole quasi-Fermi level. Since the cell voltage is the difference between electron and hole quasi-Fermi levels, and these quasi-Fermi levels have a constant offset from their respective band edges, the cell voltage differs from the bandgap voltage by a constant value, to first order.

Fig. 7 plots the measured open-circuit voltage for single-junction cells with a wide range of bandgaps, from 0.67 to 2.1 eV, against the bandgaps of the solar cell bases from quantum efficiency measurements of the absorption edge. Also plotted is the experimental bandgap-voltage offset, $(E_g/q) - V_{oc}$, and the ideal bandgap-voltage offset limited by radiative recombination. The experimental V_{oc} values closely parallel the measured E_g over the broad bandgap range, confirming that it is a good assumption that V_{oc} and E_g are related by an additive constant. At the 1.4-eV bandgap of 1%-In GaInAs, the experimental bandgap-voltage offset is nearly equal to that calculated in the radiative limit at about 370 mV, indicating that almost all of the recombination in this lattice-matched material is radiative, and only a small component is SRH recombination. Materials with higher lattice mismatch, such as 1.1-eV and 0.97-eV GaInAs have offset voltages in the 430-490 mV range, remarkably low in light of the 1.6% and 2.4% lattice mismatches of these materials, respectively.

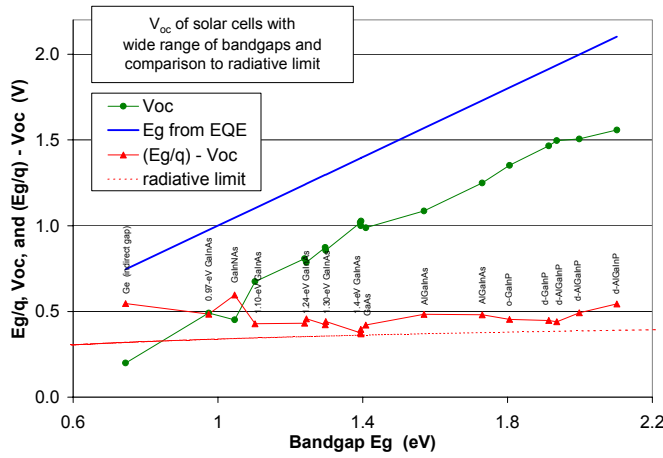


Figure 7. Experimental V_{oc} for a wide range of single-junction solar cell bandgaps, from 0.67 to 2.1 eV, showing that the bandgap-voltage offset, $(E_g/q) - V_{oc}$, is roughly constant over this range as predicted from theory. The value of this offset approaches the radiative limit for some solar cell materials.

3-junction cell results

Lattice-matched GaInP/ GaInAs/ Ge 3-junction cells have achieved the highest independently confirmed efficiency of 37.3% at 175 suns[1,19] under the AM1.5D, low-AOD spectrum, the standard reporting spectrum used by the National Renewable Energy Laboratory[18]. Metamorphic GaInP/ GaInAs/ Ge 3-junction devices, with 8%-In in the middle cell base, at a 0.5% lattice mismatch with respect to the Ge substrate, have achieved 36.9% efficiency under the same AM1.5D, low-AOD spectrum at NREL, reaching parity with the lattice-matched case in spite of the threading dislocations that can result from lattice mismatch[1].

6-junction cell results

Prototype 6-junction AlGaInP/ GaInP/ AlGaInAs/ GaInAs/ GaInNAs/ Ge cells with an active ~ 1.1 -eV GaInNAs subcell 5 have been built and tested. Measured quantum efficiencies of all six of the individual subcells for the 6-junction (6J) cell grown separately can be plotted in Fig. 8. The bandgaps of each subcell can be noted from the photon energy axis. The top subcell 1 is intentionally grown thin and transparent to light over much of its response range, in order to current match to the other subcells. The QE of the GaInNAs subcell 5, remains the most challenging. This cell is highly sensitive to annealing, including the thermal budget that the nitride cell experiences when the upper four subcells of the 6-junction cell are grown on top of it. This sensitivity is depicted in the GaInNAs cell QE measurements in Fig. 9. With a suitably low thermal budget, 8.5 mA/cm² current density can be achieved under the AM0 space spectrum, enough to current match the nitride cell to the other 6J subcells.

The measured I-V characteristics of fully-integrated 6-junction cells are shown in Fig. 10. Open-circuit voltage of 5.33 V, and preliminary efficiencies of 23.6% active-area, and 20.9% total area were measured, representing a

substantial increase over the 5.11 V and 13.47% efficiency for the first 6-junction cells tested [1]. These improvements bode well for the development of MJ cells with more than 3 junctions to increase the efficiency of terrestrial concentrator cells.

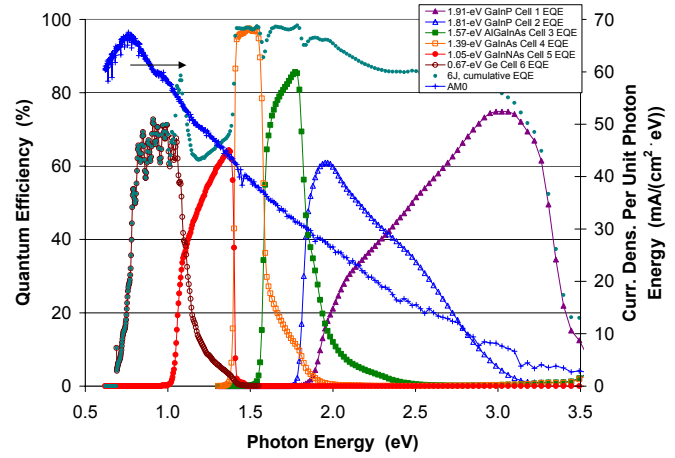


Figure 8. Quantum efficiency measurements of the six component subcells of a 6-junction solar cell, plotted vs. photon energy.

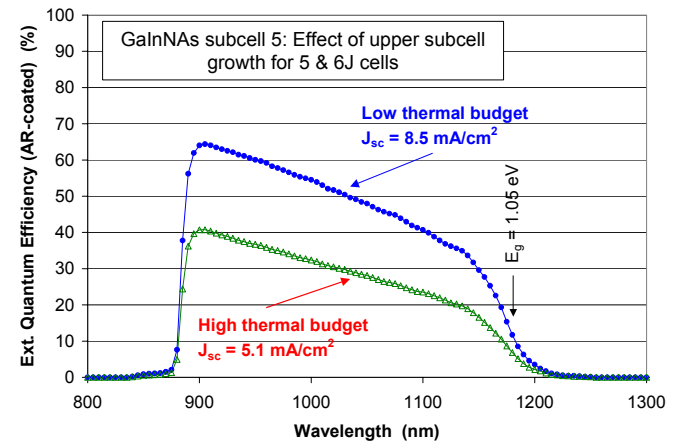


Figure 9. Measured quantum efficiency of 1.05-eV GaInNAs solar cells near the Ge lattice constant, showing the effect of thermal budget.

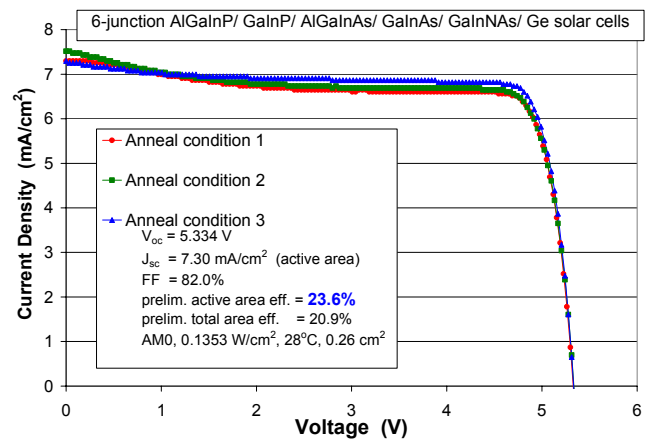


Figure 10: Illuminated current-voltage characteristics for 6-junction AlGaInP/ GaInP/ AlGaInAs/ GaInAs/ GaInNAs/ Ge solar cells, with an active ~ 1.1 -eV GaInNAs subcell 5, with V_{oc} over 5.3V.

5. Summary

The device elements for a variety of solar cell architectures capable of reaching 40% efficiency have been demonstrated. These include the use of metamorphic materials for greater freedom of bandgap selection, wider-bandgap top cell materials such as AlGaInP and alloys with a disordered group-III sublattice, and cell architectures with 3 to 6 junctions that make use of the excess current density in the Ge subcell of conventional 3-junction cells. By combining these device structure advances under investigation in research groups around the world, the goal of a practical 40%-efficient photovoltaic cell is near.

5. Acknowledgments

The authors would like to thank Martha Symko-Davies, Bob McConnell, Keith Emery, James Kiehl, Tom Moriarty, Wyatt Metzger, Richard Ahrenkiel, Brian Keyes, Manuel Romero, Dan Friedman, and Jerry Olson at NREL; and Peter Colter, Takahiro Isshiki, Moran Haddad, Kent Barbour, Mark Takahashi, and Greg Glenn, and the entire multijunction solar cell team at Spectrolab. This work was supported in part by the Dept. of Energy through the NREL High-Performance PV program (NAT-1-30620-01), by the Air Force Research Laboratory (AFRL/VS) under DUS&T contract # F29601-98-2-0207, and by Spectrolab.

6. References

[1] R. R. King, C. M. Fetzer, K. M. Edmondson, D. C. Law, P. C. Colter, H. L. Cotal, R. A. Sherif, H. Yoon, T. Isshiki, D. D. Krut, G. S. Kinsey, J. H. Ermer, Sarah Kurtz, T. Moriarty, J. Kiehl, K. Emery, W. K. Metzger, R. K. Ahrenkiel, and N. H. Karam, "Metamorphic III-V Materials, Sublattice Disorder and Multijunction Solar Cell Approaches with Over 37% Efficiency," *Proc. 19th European Photovoltaic Solar Energy Conf.*, Paris, France, 7-11 June 2004, p.3587.

[2] T. Takamoto, T. Agui, K. Kamimura, M. Kaneiwa, M. Imaizumi, S. Matsuda, and M. Yamaguchi, "Multijunction Solar Cell Technologies – High Efficiency, Radiation Resistance, and Concentrator Applications," *Proc. 3rd World Conf. on Photovoltaic Energy Conversion*, Osaka, Japan, May 11-18, 2003, p. 581.

[3] A. W. Bett, F. Dimroth, M. Hein, G. Lange, M. Meusel, U. Schubert, G. Siefer, "Development of III-V-Based Concentrator Solar Cells and Their Application in PV Modules," *Proc. 29th IEEE Photovoltaic Specialists Conf.*, New Orleans, Louisiana, May 19-24, 2002, p. 844.

[4] R. A. Sherif, R. R. King, N. H. Karam, and D. R. Lillington, "The Path to 1 GW of Concentrator Photovoltaics Using Multijunction Solar Cells," *Proc. 31st IEEE Photovoltaic Specialists Conf.*, Lake Buena Vista, Florida, Jan. 3-7, 2005, p. 17.

[5] R.A. Sherif, H.L. Cotal, R.R. King, A. Paredes, N.H. Karam, G.S. Glenn, D. Krut, A. Lewandowski, C. Bingham, K. Emery, M. Symko-Davies, J. Kiehl, S. Kusek, and H. Hayden, "The Performance and Robustness of GaInP/InGaAs/Ge Concentrator Solar Cells in High Concentration Terrestrial Modules," *Proc. 19th European Photovoltaic Solar Energy Conf.*, Paris, France, 7-11 June 2004, p. 2074.

[6] K. Araki, M. Kondo, H. Uozumi, M. Yamaguchi, "Development of a Robust and High-Efficiency Concentrator Receiver," *Proc. 3rd World Conf. on Photovoltaic Energy Conversion*, Osaka, Japan, May 11-18, 2003, p. 630.

[7] A. Bett, C. Baur, F. Dimroth, G. Lange, M. Meusel, S. van Riesen, G. Siefer, V. M. Andreev, V. D. Rumyantsev, N. A. Sadchikov, "FLATCON™-Modules: Technology and Characterisation," *Proc. 3rd World Conf. on Photovoltaic Energy Conversion*, Osaka, Japan, May 11-18, 2003, p. 634.

[8] R. M. Swanson, "The Promise of Concentrators," *Progress in Photovoltaics: Res. Appl.* **8**, pp. 93-111 (2000).

[9] R. R. King, M. Haddad, T. Isshiki, P. C. Colter, J. H. Ermer, H. Yoon, D. E. Joslin, and N. H. Karam, "Metamorphic GaInP/GaInAs/Ge Solar Cells," *Proc. 28th IEEE Photovoltaic Specialists Conf.*, Anchorage, Alaska, Sep. 15-22, 2000, p. 982.

[10] F. Dimroth, U. Schubert, and A. W. Bett, "25.5% Efficient Ga_{0.35}In_{0.65}P/Ga_{0.83}In_{0.17}As Tandem Solar Cells Grown on GaAs Substrates," *IEEE Electron Device Lett.*, **21**, p. 209 (2000).

[11] R. R. King, C. M. Fetzer, P. C. Colter, K. M. Edmondson, J. H. Ermer, H. L. Cotal, H. Yoon, A. P. Stavrides, G. Kinsey, D. D. Krut, N. H. Karam, "High-Efficiency Space and Terrestrial Multijunction Solar Cells Through Bandgap Control in Cell Structures," *Proc. 29th IEEE Photovoltaic Specialists Conf.*, New Orleans, Louisiana, May 19-24, 2002, p. 776.

[12] R. R. King, C. M. Fetzer, P. C. Colter, K. M. Edmondson, D. C. Law, A. P. Stavrides, H. Yoon, G. S. Kinsey, H. L. Cotal, J. H. Ermer, R. A. Sherif, K. Emery, W. Metzger, R. K. Ahrenkiel, and N. H. Karam, "Lattice-Matched and Metamorphic GaInP/GaInAs/Ge Concentrator Solar Cells," *Proc. 3rd World Conf. on Photovoltaic Energy Conversion*, Osaka, Japan, May 11-18, 2003, p. 622.

[13] C. M. Fetzer, R. R. King, P. C. Colter, K. M. Edmondson, D. C. Law, A. P. Stavrides, H. Yoon, J. H. Ermer, and N. H. Karam, "High-efficiency GaInP/GaInAs/Ge solar cells grown by MOVPE," *J. Crystal Growth*, **261**, pp. 341-348 (2004).

[14] C. M. Fetzer, H. Yoon, R. R. King, D. C. Law, T. D. Isshiki, and N. H. Karam, "1.6/1.1 eV metamorphic GaInP/GaInAs solar cells grown by MOVPE on Ge," *J. Crystal Growth*, **276**, pp. 48-56.

[15] D. C. Law, C. M. Fetzer, R. R. King, P. C. Colter, H. Yoon, T. D. Isshiki, K. M. Edmondson, M. Haddad, and N. H. Karam, "Multijunction Solar Cells with Subcell Materials Highly Lattice-Mismatched to Germanium," *Proc. 31st IEEE Photovoltaic Specialists Conf.*, Lake Buena Vista, Florida, Jan. 3-7, 2005, p. 575.

[16] J. C. Schultz, M. E. Klausmeier-Brown, M. Ladle Ristow, and M. M. Al-Jassim, "High Efficiency 1.0-eV GaInAs Bottom Solar Cell for 3-Junction Monolithic Stack," *Proc. 21st IEEE Photovoltaic Specialists Conf.*, Kissimmee, Florida, May 21-25, 1990, p. 148.

[17] M. W. Wanlass, S. P. Ahrenkiel, R. K. Ahrenkiel, D. S. Albin, J. J. Carapella, A. Duda, J. F. Geisz, Sarah Kurtz, T. Moriarty, R. J. Werner, and B. Wernsman, "Lattice-Mismatched Approaches for High-Performance, III-V, Photovoltaic Energy Converters," *Proc. 31st IEEE Photovoltaic Specialists Conf.*, Lake Buena Vista, Florida, Jan. 3-7, 2005, p. 530.

[18] K. Emery, D. Meyers, and Sarah Kurtz, "What is the Appropriate Reference Spectrum for Characterizing Concentrator Cells?," *Proc. 29th IEEE Photovoltaic Specialists Conf.*, New Orleans, Louisiana, May 19-24, 2002, pp. 840-843.

[19] M. A. Green, K. Emery, D. L. King, S. Igari, W. Warta, "Solar Cell Efficiency Tables (Version 24)," *Progress in Photovoltaics: Res. Appl.* **12**, pp. 365-372 (2004).